
Inline 3D X-ray Inspection of Food using Discrete Tomography

Luis F. A. Pereira, Tom Roelandts, Jan Sijbers

iMinds-Vision Lab, University of Antwerp, Universiteitsplein 1, 2610 Wilrijk (Antwerp), Belgium

ABSTRACT

While X-ray radiography is commonly used for inline inspection of food, it is insufficient if 3D information is needed from the scanned object. Computed Tomography (CT) on the other hand, does provide 3D information, but is known to be expensive and relatively slow.

This work proposes a low-cost X-ray scanning system based on a static X-ray source with a wide cone, along with a large detector with which only few projections are acquired while food passes by on a conveyor belt. For such scanning geometry, conventional tomographic reconstruction methods would lead to images that are severely polluted with smearing artefacts. In this paper, we propose the use of the Discrete Algebraic Reconstruction Technique (DART) to reduce these artefacts. Simulation results show that DART can generate reconstructions of much higher quality than conventional reconstruction methods in conveyor belt X-ray scanning which is an important step towards quantitative analysis of 3D objects for inline X-ray inspection.

1 Introduction

Conventional X-ray scanning has been extensively used in food inspection for detecting defects and contaminants (Bull, Zwiggelaar and Speller, 1997; Mery *et al.*, 2011; Lammertyn *et al.* 2012). However, traditional X-ray radiography cannot be used to extract quantitative 3D information about the scanned object. Computed Tomography (CT), in which multiple projections are acquired from the target object and then mathematically combined, is more suited for this purpose. Unfortunately, CT systems are expensive, and suffer from long acquisition times. Moreover, the image reconstruction process associated with CT technology does not allow scanning a large number of objects in an industrial scale as conventional X-ray systems are used today. However, if the technology improves, CT scanning can replace traditional X-ray imaging as the predominant method for real time food inspection (Haff and Toyofuku, 2008).

To make CT scanning cheaper and faster, this work proposes a system based on a static setup consisting of a wide cone X-ray source and a large detector for imaging food passing by on a conveyor belt. In order to reduce the time needed for the image reconstruction process, only a limited number of projections is acquired. In this scenario, the constraints associated to the imaging angular range and to the number of available projections would lead to significant smearing artefacts if conventional reconstruction techniques are used. Therefore, a recently proposed reconstruction method, the Discrete Algebraic Reconstruction Technique (DART), is used (Batenburg and Sijbers, 2011). DART has successfully been applied in electron and X-ray diffraction tomography (Batenburg *et al.*, 2009; Batenburg *et al.*, 2010). It incorporates specific prior knowledge related to the scanned object and it has shown to reconstruct high quality images, reducing the occurrence of smearing artefacts, even from a limited amount of data.

This paper is organized as follows: Section 2 describes the theory related to the techniques used in this work, Section 3 presents the experiments which were conducted, Section 4 exposes the obtained results and a brief discussion about them, and Section 5 contains the final conclusion.

2 Material and Methods

In this section, the X-ray conveyor belt geometry and its constraints are exposed in Subsection 2.1. Next, a brief introduction to Algebraic Reconstruction is given in Subsection 2.2. Then, DART is detailed in Subsection 2.3.

2.1 X-ray conveyor belt geometry

The proposed setup for scanning is composed by a wide cone beam X-ray source, a large detector, and a conveyor belt. Fig. 1 illustrates how these elements are arranged to compose the geometry: the X-ray source (a)

is positioned above the conveyor belt (b) at a distance D , and the detector (c), of length K , is centralized according to (a) and just below to (b).

This static setup allows cheaper and faster scanning compared to conventional CT systems in which the X-ray source and the detector rotate around the target object. However, it imposes a strong constraint relative to the angular range for object imaging which may lead to significant smearing artefacts in the reconstructed image. In fact, the available angular range (α) for food imaging can be calculated from D and K according to the relation exposed in Eq. (1).

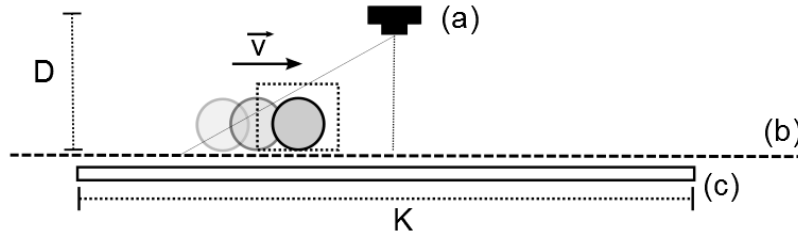


Fig. 1 The conveyor belt X-ray geometry.

$$\alpha = 2 \tan^{-1} \left(\frac{K/2}{D} \right) \quad (1)$$

2.2 Algebraic Reconstruction

The Algebraic Reconstructions Methods (ARM) considers the image reconstruction problem as the solving of a system of linear equations. Let v be a discretized object function which represents a grid of pixels of the reconstructed image and let p be the vector containing the projection data of the scanned object. Then, p and v are related by the following equation:

$$p = Wv \quad (2)$$

where W is called the *projection matrix* and maps a vector from the reconstruction domain into the projection domain. It can be computed, for example, using a line-kernel projector model in which w_{ij} is defined by the length of a single detector line i through the pixel j (Siddon, 1985). Finally, the solution can be found by the minimization of the following function (Buzug, 2008):

$$\chi^2 = |Wv - p|^2 \quad (3)$$

2.3 Discrete Algebraic Reconstruction Technique (DART)

DART is an algebraic reconstruction method for image reconstruction based on the interleaving of continuous update steps and discretization steps, which incorporates prior knowledge relative to the expected density of the scanned material. The flow chart of Fig. 3 shows the sequence of stages which compose the DART algorithm. Then, each DART stage is explained in detail:

- **Compute an initial ARM reconstruction:** DART starts with an initial reconstruction of the acquired data p obtained with a continuous iterative reconstruction algorithm, such as ART (Buzug, 2008), SART (Andersen and Kak, 1984) or SIRT (Gregor and Benson, 2008).
- **Segment the reconstruction:** the reconstruction is segmented according to the set of grey values $(\rho_1, \rho_2, \dots, \rho_\ell)$ that is expected for the image. In fact, since the grey values of the reconstructed image are associated with the attenuation values of the target object in each region, this incorporated prior knowledge is related to the expected density of the materials of which the object is composed. In this stage, $\ell - 1$ thresholds (τ_i) are applied to the image, defined as

$$\tau_i = \frac{\rho_i + \rho_{i+1}}{2} \quad (4)$$

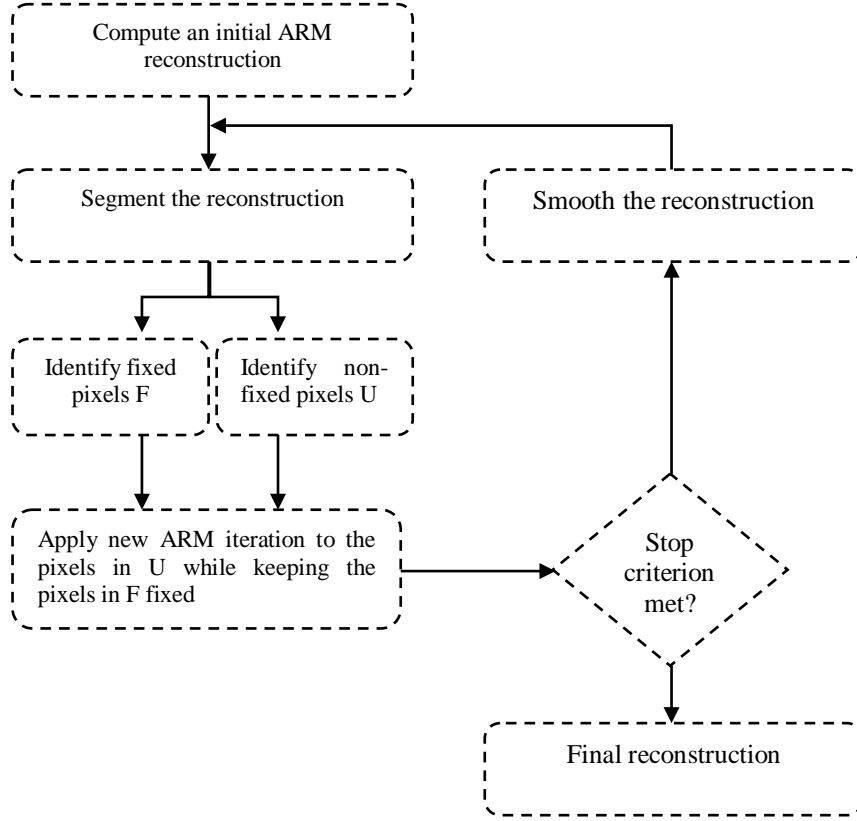


Fig. 3 Flow chart of DART algorithm.

- **Identify non-fixed pixels U:** Let $U^{(k)} \subset \{1, 2, \dots, n\}$ be the set of pixels to be updated in the k th iteration of DART. Since experimental results showed that ARM leads to errors near the edges of the reconstructed image, all boundary pixels of the current segmented image are thus added to $U^{(k)}$. For this purpose, every pixel whose value is different from at least one of its neighbouring pixels is considered a boundary pixel. Moreover, each non-boundary pixel is added to $U^{(k)}$ with a certain probability $0 \leq r \leq 1$. In this way, the accuracy of DART reconstruction is increased in case of small holes or features which were missed during the initial reconstruction.
- **Identify fixed pixels F:** The complementary pixels set $F^{(k)} = \{1, 2, \dots, n\} \setminus U^{(k)}$ contains all the pixels that will be removed from the reconstruction problem for the next ARM iteration.
- **Apply new ARM iterations to the pixels in U while keeping the pixels in F fixed:** Expanding Eq. (2), one can write:

$$p = \begin{pmatrix} \vdots & \vdots & \vdots \\ w_1 & \cdots & w_n \\ \vdots & \vdots & \vdots \end{pmatrix} \cdot \begin{pmatrix} v_1 \\ \vdots \\ v_n \end{pmatrix} \quad (5)$$

where w_j denotes the j th column of the matrix W . By removing the j th fixed pixel from v , the reconstruction equation is updated to Eq. (6). Then, an ARM iteration is applied for this new linear

system which has the same number of equations and a lower number of variables.

$$p - w_j v_j = \begin{pmatrix} \vdots & \vdots & \vdots & \vdots & \vdots & \vdots \\ w_1 & \cdots & w_{j-1} & w_{j+1} & \cdots & w_n \\ \vdots & \vdots & \vdots & \vdots & \vdots & \vdots \end{pmatrix} \cdot \begin{pmatrix} v_1 \\ \vdots \\ v_{j-1} \\ v_{j+1} \\ \vdots \\ v_n \end{pmatrix} \quad (6)$$

- **Stop criterion met:** The consecutive iterations of DART can be stopped according to the convergence of the *total projection error*, described in Eq. (6), or based on a fixed number of iterations.
- **Smooth the reconstruction:** Reducing the number of variables by selecting a subset of non-fixed pixels $U^{(k)}$ may lead to more noise sensitive ARM reconstructions. Then, a Gaussian smoothing filter is applied to the boundary pixels after applying the ARM.

DART results in better reconstructions by reducing the number of unknowns according to Eq. (6). Therefore, the selection of pixels to be updated from the segmented image, which is based on the prior knowledge of the grey levels, plays a fundamental role in this approach.

3 Experiments

Simulation experiments were conducted to evaluate the quality of SIRT and DART reconstructions in the X-ray conveyor belt scanning system. The investigated scenarios included several configurations for the detector size, which led to meaningful variations in the available angular range for imaging the target object. More precisely, the size of detector was varied from 40 cm to 160 cm while only 25 projections were used. Furthermore, the quality of the reconstructions was also evaluated when different numbers of projections were used, which is directly associated with the time needed to compute the reconstructed image. For this purpose, the detector size was 90 cm.

All the projections used in this work were generated from a CT image of a cross section of pear (Lammertyn *et al.*, 2003), shown in Fig. 4, which was stored for 72 days after harvest. Some cavities formed in the tissue due to storage disorder can be already seen.

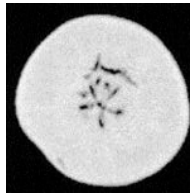


Fig. 4 CT reconstruction of a cross section of pear used to generate projections.

4 Results and Discussion

Fig. 5 shows the reconstructed images obtained using SIRT and DART in the X-ray conveyor belt scanning system for different detector sizes ($K = 41.6$ cm, $K = 72.8$ cm and $K = 104$ cm) and 25 projections. Next, Fig. 6 shows the obtained results when the number of projections is varied ($N = 4$, $N = 16$ and $N = 64$) when a detector of 90 cm is used. Finally, the results for an entire range of detector sizes and number of projections are shown in Fig. 7, where the Mean Squared Error (MSE) of the reconstructions in relation to the original image are plotted.

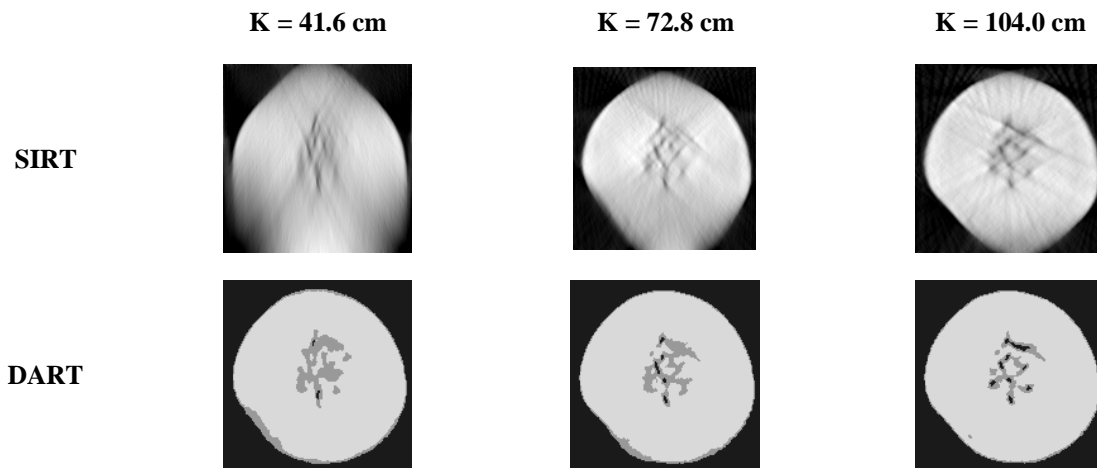


Fig. 5 Reconstructions of a cross section of pear obtained using SIRT and DART in the X-ray conveyor belt geometry for different detector sizes.

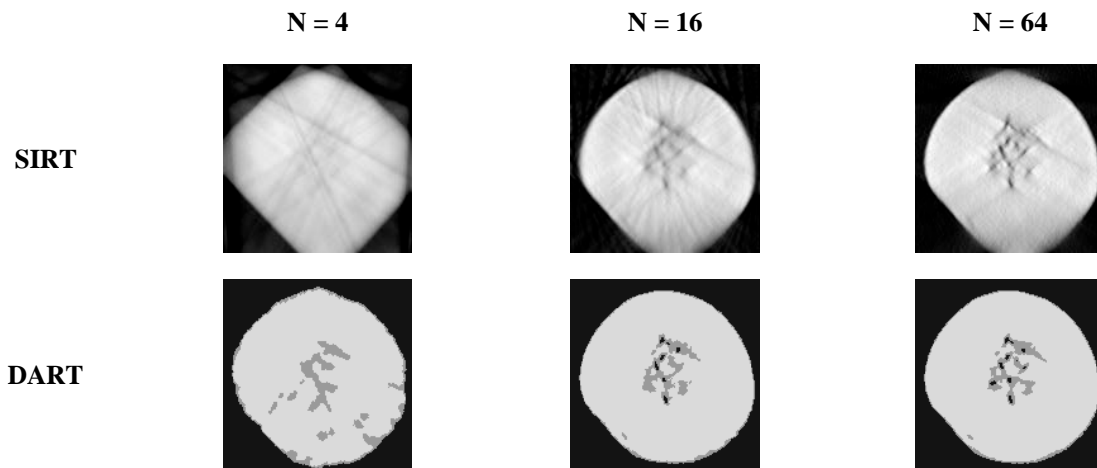


Fig. 6 Reconstructions of a cross section of pear obtained using SIRT and DART in the X-ray conveyor belt geometry for different number of projections.

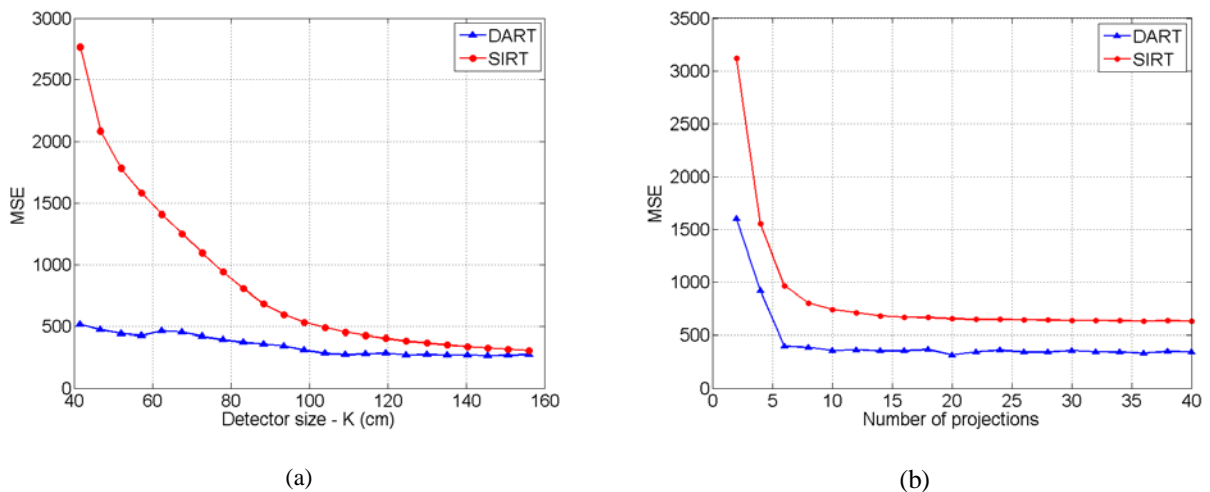


Fig. 7 MSE of the reconstructions obtained using DART and SIRT in the X-ray conveyor belt geometry for different detector sizes (a) and different numbers of projections (b).

The results show that DART can reconstruct images of similar quality as ARM, using half the detector size. This result implies that a much cheaper system is possible. In fact, using a detector of length up to 60 cm,

the error associated with the DART reconstructions is, at least, 3 times smaller than that obtained with the conventional method.

Moreover, DART is better suited to perform reconstructions from a lower number of projections, which leads to faster CT systems. More precisely, using a detector of 90 cm, DART achieves good quality reconstructions from only 6 projections.

5 Conclusions

This work shows that DART is suited to operate within the constraints imposed by the X-ray conveyor belt geometry. Moreover, it was shown that the use of prior knowledge on the number of grey levels with which the reconstruction can be represented can overcome smearing artefacts associated with a limited angular range and a reduced number of projections used in such acquisition geometry.

Acknowledgements

The work presented in this paper was financially supported by the Institute for the Promotion of Innovation through Science and Technology in Flanders (IWT Vlaanderen) through the SBO project TOMFOOD and by iMinds.

References

- Andersen, A. H. and Kak, A. C., 1984. Simultaneous Algebraic Reconstruction Technique (SART): a superior implementation of the ART algorithm. *Ultrason. Img.*, vol. 6, pp. 81-84.
- Batenburg, K. J., Bals, S., Sijbers, J., Kubel, C., Midgley, P. A., Hernandez, J. C., Kaiser, U., Encina, E. R., Coronado, E. A., and Van Tendeloo, G., 2009. 3D imaging of nanomaterials by discrete tomography", *Ultramicroscopy*, vol. 109, pp. 730-740.
- Batenburg, K. J., Sijbers, J., Poulsen, H. F., and Knudsen, E., 2010. DART: A Robust Algorithm for Fast Reconstruction of 3D Grain Maps, *Journal of Applied Crystallography*, vol. 43, pp. 1464-1473.
- Batenburg, K. J. and Sijbers, J., 2011. DART: A practical reconstruction algorithm for discrete tomography. *IEEE Transactions on Image Processing*, vol. 20, no. 9, pp. 2542-2553.
- Bull, C. R., Zwiggelaar, R. and Speller, R. D., 1997. Review of inspection techniques based on the elastic and inelastic scattering of the X-rays and their potential in the food and agricultural industry. *Journal of Food Engineering*, vol. 33, pp. 167-179.
- Buzug, T. M., 2008. *Computed Tomography: From Photon Statistics to Modern Cone-Beam CT*. Springer-Verlag Berlin Heidelberg.
- Gregor, J. and Benson, T., 2008. Computational analysis and improvement of SIRT. *IEEE Transactions on Medical Imaging*, vol. 27, no. 7, pp. 918-924.
- Haff, R. P. and Toyofuku, N., 2008. X-ray detection of defects and contaminants in the food industry. *Sensory and Instrumentation for Food Quality*, no 2, pp. 262-273.
- Lammertyn, J., Dresselaers, T., Van Hecke, P., Jancsó, P., Wevers, M., Nicolai, B. M., 2003. Analysis of the time course of core breakdown in 'Conference' pears by means of MRI and X-ray CT. *Postharvest Biology and Technology*, vol. 29, pp. 19-28.
- Mery, D., Lillo, I., Loebel, H., Rizzo, V., Soto, A., Cipriano, A., Aguilera, J. M., 2011. Automated fish bone detection using X-ray imaging. *Journal of Food Engineering*, vol. 105, pp. 485-492.
- Siddon, R. L., 1985. Fast calculation of the exact radiological path for a three-dimensional ct array. *Medical Physics*, vol. 12, no. 2, pp. 252-255.